Supporting Information

"Catalysis by Alkaline Phosphatase is Ultrasensitive to Charge Sequestered Between the Active Site Zinc Ions in the Transition State"

Ivana Nikolic-Hughes, Patrick J. O'Brien, Daniel Herschlag
Departments of Chemical Engineering, Chemistry and Biochemistry, Stanford University, Stanford, CA 94305

Supporting Methods:

The following Supporting Methods describe determination of the charge density on each non-bridging oxygen atom and catalytic proficiencies for the R166S AP-catalyzed reactions of the following substrates: *para*-nitrophenyl phosphate (pNPP), *para*-nitrophenyl phosphorothioate (pNPPS), *bis*-(*para*-nitrophenyl) phosphate (bpNPP), methyl *para*-nitrophenyl phosphate (MpNPP), methyl *para*-nitrophenyl phosphorothioate (MpNPPS), *para*-nitrophenyl sulfate (pNPS) and di-ethyl *para*-nitrophenyl phosphate (dEpNPP). These values are summarized in Table 1 in the main text and used in the correlation of Fig. 1 in the main text.

1. Determination of Charge Density on the Non-bridging Atoms of AP Substrates

Phosphate and Sulfate Esters: Non-bridging Oxygen Atom Charge Density. The ground state charges on the non-bridging oxygen atom of phosphate and sulfate esters (pNPP, bpNPP, MpNPP, dEpNPP and pNPS) were calculated as follows: total atomic charge of the substrate was simply divided by the total number of non-bridging oxygen atoms in the molecule. More sophisticated approaches have been used to determine charges on individual atoms of these substrates (ref. S1). Although differences in charge values exist between these methods, they are small enough so as not to affect any of the results or conclusions.

Phosphorothioate Esters: Empirical and Computational Methods for Charge Density Determination. Frey and Sammons (ref. S2) have suggested that phosphorothioate anions contain nearly a single P-S bond with negative charge preferentially localized on the sulfur atom, while the P-O bond order for non-bridging oxygen atoms is significantly greater than one. Their conclusions are supported by bond lengths obtained from crystallographic data, electron diffraction, pK_a values for phosphoric and thiophosphoric acids, vibrational spectra of thiophosphate di- and trianions, the pH-dependence of ^{17}O-nuclear magnetic resonance (NMR) chemical shifts in [^{17}O]phosphate and [^{17}O]thiophosphate, and the magnitude of the effects of ^{18}O atoms on the ^{31}P-NMR chemical shifts of phosphorus in nucleoside [^{18}O]phosphorothioates (see ref. S2).

It has previously been determined that a proportionality relationship exists between the magnitude of the ^{31}P-NMR chemical shift for ^{18}O-bonded phosphates relative to ^{16}O-bonded species ($\Delta\delta_p$) and P-O bond order for the ^{18}O-atom (ref. S3). Frey and Sammons used this approach to calculate P-O bond orders for nucleoside phosphorothioates. A summary of their

results for adenosine monothiophosphate (AMPS) and adenosine α–thiodiphosphate ($ADP_\alpha S$) is presented in Table S1. The data for S-methyl adenosine monothiophosphate (S-methyl AMPS), the compound that defines the relationship between $\Delta\delta_p$ and the P-O bond order, is also included in Table S1.

We determined the negative charge on the non-bridging oxygen and sulfur atoms of AMPS and $ADP_\alpha S$ using the relationship: Charge = Bond Order - 2 (ref. S1). The results for AMPS, which we use as a model monosubstituted phosphorothioate, are summarized in Table S2 and the results for $ADP_\alpha S$, which we use as a model disubstituted phosphorothioate, are summarized in Table S3.

Liang and Allen (ref. S1) calculated the charges in phosphorothioate anions (thiophosphoric acids) using two different methods: Mulliken population analysis at optimized geometries and molecular electrostatic potential analysis. Their findings for the dianionic thiophosphoric acid are also summarized in Table S2 and their findings for the monoanionic thiophosphoric acid are summarized in Table S3 alongside the empirical results.

The last row in Tables S2 and S3 gives average values of charge and bond order obtained by the empirical and computational methods. In the light of limitations of these methods, as applied to our aryl phosphorothioate esters, we have used the average value for the non-bridging oxygen charge in the correlation of Fig.1 in the main text. The range of charge values for phosphorothioate esters arising from the empirical and two computational methods is smaller than the size of the symbols in Fig. 1. Moreover, using charges obtained by any one of the different methods gives correlation slopes that are within 15% of the value obtained by using average charge, and do not alter any of the conclusions.

Table S1. Summary of the Empirical Method for P-O and P-S Bond Order Determination. Data from ref. S2.

Compound		$\Delta\delta_p$ *(ppm)*[a]	*Bond Order*[b]	
			P-O	*P-S*
S-methyl AMPS	Reference	0.035	1.500	1.000
AMPS	Monoester Model	0.033	1.414	1.172
$ADP_\alpha S$	Diester Model	0.037	1.585	1.415

[a]Magnitude of the ^{31}P-NMR chemical shift for ^{18}O-bonded relative to ^{16}O-bonded phosphates.
[b]Bond order of non-bridging bonds, except for the P-S bond of S-methyl AMPS, which is a bridging bond, assuming a total bond order of five and bond orders of one for all bridging atoms. The sulfur atom of S-methyl AMPS is methylated and is used as the control that defines a P-S bond order of 1. The bond order for the two remaining P-O non-bridging bonds in S-methyl AMPS is therefore equal to 1.5 [(5-2)/2], as the third P-O bond is also bridging and has a bond order of 1.

Table S2. Bond Order and Charge of Monosubstituted Phosphorothioates.

Method	*Bond Order*[a]		*Charge*		*Total atomic charge*[b]
	P-O	*P-S*	*O-atom*	*S-atom*	
Empirical[c]	1.414[d]	1.172[d]	-0.586[e]	-0.828[e]	-2.002
Mulliken[f]	1.400	1.240	-0.600	-0.760	-2.160
Electrostatic potential[f]	1.380	1.300	-0.620	-0.700	-1.940
Overall average	1.402±0.012	1.22±0.05	-0.598±0.012[g]	-0.78±0.05	-2.02±0.13

[a]For non-bridging P-O and P-S bonds.
[b]Calculated by summation of two oxygen atom charges and one sulfur atom charge.
[c]Reference S2.
[d]Values for AMPS, the monoester model compound are from Table S1.
[e]Calculated using the following relationship: [Charge = Bond Order – 2] (ref. S1).
[f]Values from reference S1.
[g]Charge value used in the correlation of Fig. 1 in the main text.

Table S3. Bond Order and Charge of Disubstituted Phosphorothioates.

Method	*Bond Order*[a]		*Charge*		*Total atomic charge*[b]
	P-O	*P-S*	*O-atom*	*S-atom*	
Empirical[c]	1.585[d]	1.415[d]	-0.415[e]	-0.585[e]	-1.00
Mulliken[f]	1.510	1.390	-0.490	-0.610	-1.10
Electrostatic potential[f]	1.500	1.440	-0.500	-0.560	-1.06
Overall average	1.545±0.045	1.415±0.025	-0.455±0.04[g]	-0.585±0.025	-1.04±0.065

[a]For non-bridging P-O and P-S bonds.
[b]Calculated by summation of one oxygen atom charge and one sulfur atom charge.
[c]Reference S2.
[d]Values for AMPS, the monoester model compound are from Table S1.
[e]Calculated using the following relationship: [Charge = Bond Order – 2] (ref. S1).
[f]All values are taken from reference S1.
[g]Charge value used in the correlation of Fig. 1 in the main text.

2. Determination of Catalytic Proficiencies for R166S AP-Catalyzed Reactions

The nonenzymatic and enzymatic rate constants, taken from the literature or determined in this work, are shown in Table S4, along with the temperature at which the reactions were performed. The resulting catalytic proficiencies for each of the substrates are also listed.

Nonenzymatic Hydrolysis of pNPS. Standard reaction conditions for nonenzymatic hydrolysis of pNPS were 0.1 M NaMOPS, pH 9.0, 0.5 M NaCl and 30 ºC. The reaction was followed in the pH-independent region, to insure that S-O bond cleavage was monitored (reference S4). The appearance of the phenolate product was monitored continuously using a Uvikon XL spectrophotometer at 410 nm. The uncatalyzed second-order rate constant, k_{water}, was determined from initial rates ($\leq$2% reaction), and the reactions were shown to be first order in substrate by varying substrate concentration 8-fold. The rate constant reported in Table S4 agrees within error with that previously published by Benkovic and Benkovic (reference S4), using the published temperature dependence.

R166S AP purification. R166S AP was purified as was reported previously (reference S5), and used in enzymatic hydrolysis reactions of pNPPS and dEpNPP. For reactions with MpNPP, MpNPPS and pNPS, a protein of still higher purity was prepared using a protein fusion and purification system from New England Biolabs (NEB), that utilizes a gene encoding for the maltose-binding protein. The construction of the fusion plasmid (R166S – pMal-p2x) was performed as described in the NEB protocol (reference S6). After the plasmid was established in a non-expression host, it was transformed into the E. coli SM547 (DE3) host bearing the T7 RNA polymerase gene (DE3 lysogen). The *E. coli* strain SM547 was lysogenized using the λ DE3 lysogenization kit from Novagen (ref. S7). The purification protocol was modified from that previously described (reference S5). The SM547 (DE3) cells harboring the R166S AP - pMal plasmid were grown in 2 L of rich medium + glucose + 100 μg/mL ampicillin. 0.3 mM IPTG was added when the cells reached and OD of ~0.5. Growth was continued for 8 hours. Following osmotic shock and centrifugation, the supernatant was adjusted to 1 mM $MgCl_2$, 100 μM $ZnSO_4$, and 10 mM Tris (pH 7.5), and loaded onto a 50 mL amylose column (column buffer 20 mM Tris, 200 mM NaCl, 1 mM $MgCl_2$, 100 μM $ZnSO_4$). The sample was eluted with column buffer plus 10 mM maltose. Peak fractions were pooled and this sample was desalted on a 10 mL desalting column (Pharmacia), then loaded onto a 50 mL Source Q column (Pharmacia). The Source Q column was washed with four column volumes of buffer A [10 mM Tris (pH 7.4), 100 μM $ZnSO_4$, and 1 mM $MgCl_2$], and eluted with a linear gradient of 0 to 200 mM NaCl in buffer A over 10 column volumes. Following concentration by centrifugation through a filter (50 kDa cutoff, Amicon), the sample was loaded onto a gel filtration column (Sephacryl S300) and run with 0.1 M NaMOPS (pH 8.0), 1 mM $MgCl_2$, and 100 μM $ZnSO_4$. Peak fractions were pooled and concentrated to <1mL by centrifugation through a filter (50 kDa cutoff, Amicon). Protein concentration was determined via an activity assay with saturating pNPP, using the value of k_{cat}= 1 s^{-1}.

Enzymatic Hydrolysis of pNPPS, MpNPP, MpNPPS and pNPS. Standard reaction conditions for enzymatic hydrolysis of pNPPT, MpNPP, MpNPTP and pNPS were 0.1 M NaMOPS, pH 8.0, 0.5 M NaCl, 100 μM $MgCl_2$, and 10 μM $ZnSO_4$ at 25 or 30 ºC (see Table S4). The appearance of the phenolate product was monitored non-continuously and/ or continuously using

a Uvikon XL spectrophotometer at 410 nm. Rate constants were obtained from initial rates (≤5% reaction). Product formation was linear in all cases. Reactions were shown to be first order in substrate and enzyme by varying substrate concentration over a range of 6-10 fold and enzyme concentration from 10-100 μM. The apparent second order rate constants, k_{cat}/K_M, are reported per active site in Table S4. To confirm that the R166S AP mutant activities were monitored, and not those of contaminating wt AP or other enzyme, 400 μM of inorganic phosphate was added to each reaction. The rate constants obtained in this background were ~2-fold lower, within error, indicating that the K_i for inorganic phosphate was ~ 400 μM, as was previously determined for R166S AP (ref. S14).

Catalytic Proficiency Limit for Hydrolysis of dEpNPP. To determine the catalytic proficiency for diethyl *p*-nitrophenyl phosphate (dEpNPP), 0.1-10 mM substrate was first incubated in 0.1 M NaMOPS, pH 8.0, 0.5 M NaCl, at 25 °C, for sufficient time to observe the background rate of hydrolysis. The reactions were repeated with addition of 100 μM $MgCl_2$, 10 μM $ZnSO_4$ and up to 100 μM R166S AP. No change in the initial rates was observed upon enzyme addition, compared to the background reactions. Control reactions with pNPP established that R166S AP maintained full activity over these time courses. No inhibition of pNPP hydrolysis with R166S AP was observed for concentrations of dEpNPP up to 10 mM.

The two possible paths for dEpNPP hydrolysis are represented in Scheme S1. The limit for the catalytic proficiency for reaction of dEpNPP was obtained as follows.

Scheme S1.

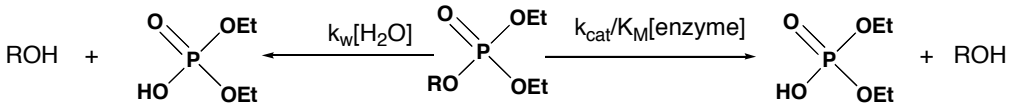

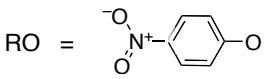

According to Scheme S1, the observed rate constant for the reaction in the presence of enzyme is equal to the sum of the rate constants for the two pathways, nonenzymatic hydrolysis and enzymatic hydrolysis:

$$k_{obs} = k_w[H_2O] + \frac{k_{cat}}{K_M}[enzyme] \qquad \text{(Eq. S1)}$$

Eq. S1 can be rearranged to yield an expression that contains the ratio of the enzymatic and nonenzymatic second-order rate constants:

$$\frac{k_{obs}}{k_w[H_2O]} = 1 + \frac{\frac{k_{cat}}{K_M}[enzyme]}{k_w[H_2O]} \qquad \text{(Eq. S2)}$$

Since a 20% rate enhancement would have been readily detected, Eq. S2 simplifies to:

$$\frac{k_{obs}}{k_w[H_2O]} \leq 1.2 \qquad \text{(Eq. S3)}$$

$$0.2\,\frac{[H_2O]}{[enzyme]} \geq \frac{\frac{k_{cat}}{K_M}}{k_w} \qquad \text{(Eq. S4)}$$

From Eq. S4, for a reaction containing 55 M water and 100 μM enzyme, the upper limit for the catalytic proficiency $[(k_{cat}/K_M)/k_w]$ is $1.1 \bullet 10^5$.

Table S4. Nonenzymatic and Enzymatic Rate Constants for Phosphate and Sulfate Esters[a]

Substrate	k_w (M^{-1} s^{-1})	k_{cat}/K_M (M^{-1} s^{-1})	$Log[(k_{cat}/K_M) / k_w]$
PNPP	$3.0 \cdot 10^{-11}$ (b)	$1.0 \cdot 10^{5}$ (c)	15.5
PNPPS	$2.0 \cdot 10^{-10}$ (d)	$2.6 \cdot 10^{3}$	13.1
MpNPP	$4.7 \cdot 10^{-12}$ (e)	$1.5 \cdot 10^{0}$	11.5
b(pNP)P	$7.3 \cdot 10^{-13}$ (f)	$5.0 \cdot 10^{-2}$ (g)	10.8
MpNPPS	$8.2 \cdot 10^{-13}$ (h)	$3.9 \cdot 10^{-2}$	10.7
PNPS	$2.0 \cdot 10^{-11}$	$3.2 \cdot 10^{-4}$	7.2
dEpNPP	$5.5 \cdot 10^{-10}$ (i)	$< 6.0 \cdot 10^{-5}$ (j)	< 5

(a) Catalytic proficiency of MpNPP, MpNPPS and pNPS was determined at 30 ºC, rather than at 25 ºC, as for the other substrates, but control reactions with pNPS at 25 ºC show that the difference in Log [(k_{cat}/K_M) / k_w] between the two temperatures is ~ 0.1 Log unit. This small difference does not affect the results or conclusions.

(b) From reference S8.

(c) From reference S9.

(d) From reference S10, using the published temperature dependence.

(e) The nonenzymatic rate constant for MpNPP was estimated using the second-order rate constant for phenoxide attack on MpNPP at 39 ºC from reference S11, and correcting it for temperature using the temperature dependence for bis(pNP)P hydrolysis from reference S12, and for nucleophilic pK_a(ΔpK_a=11.7) using a β_{nuc} of 0.31, as determined by Kirby and Younas (reference S13). The rate constant thus calculated agrees within error with that measured recently for hydroxide attack on MpNPP (Jesse Zalatan & DH, unpublished results).

(f) From reference S12, using the published temperature dependence.

(g) From reference S14.

(h) The nonenzymatic rate constant for MpNPPS was estimated using the rate constant for MpNPP (see above) and the thio effect of 7 (see reference S15).

(i) The nonenzymatic rate constant for dEpNPP was estimated using the second-order rate constant for hydrolysis of diethyl 2,4 dinitorphenyl phosphate from reference S16, and correcting it for leaving group pK_a, using the leaving group dependence for phenoxide attack on diethyl aryl phosphates from reference S11.

(j) Calculated from the nonenzymatic rate constant k_w (see footnote i) and the limit on catalytic proficiency, which was determined as described in the Supporting Methods.

Supporting Discussion:

We have considered several explanations for the large observed differences in the catalytic proficiencies of AP for its various activities. To test possible factors, we assessed several correlations between the catalytic proficiency of AP and substrate features, and we compared these correlations to that for estimated charge on the non-bridging oxygen atom(s) that is presented in the main text.

In Figure S1, the log of the catalytic proficiency is plotted against the total charge on the substrate. The data fit by a single correlation line give a value of R^2 equal to 0.63. This correlation coefficient is significantly lower than that for the correlation between catalytic proficiency and the non-bridging oxygen atom charge, discussed in the main text ($R^2 = 0.98$). Although greater total charge may result in increased binding to the positively charged active site, it does not appear to best account for the discrimination by AP between different substrates.

We next investigated the relationship between the log of the AP catalytic proficiency with the bond length of the P-O (S-O) non-bridging bond (Figure S2). The data fit by a single correlation line give a value of R^2 equal to 0.63. This correlation coefficient is also significantly lower than that for the correlation between catalytic proficiency and the non-bridging oxygen atom charge, discussed in the main text ($R^2 = 0.98$), suggesting that charge dominates over any length effect.

Lastly, we determined if there is a correlation between the substrate transition state character and the AP catalytic proficiency. We used two different values to describe the transition state character, the α-value, which measures fractional bond cleavage (Table S5 and Figure S3) and β_{lg}, which measures the change in charge between the ground state and the transition state (Table S6 and Figure S4). The data fit by a single correlation line give R^2 equal to 0.05 in both cases. Such poor correlation coefficients suggest that transition state character does not appear to account well for the discrimination by AP between different substrates.

Table S5. α-Values in Solution for AP Substrates

Substrate	*Nucleophile*	β_{lg}	*Nucleophile*	β_{eq}	$\alpha = \beta_{lg} / \beta_{eq}$
pNPP	Water	-1.23[a]	Water	-1.35[b]	0.91
PNPPS	Water	-1.15[c]			
b(pNP)P	Hydroxide	-0.8[d]	Phenoxide	-1.74[e]	0.46
MpNPP	Hydroxide	-0.8[d]	Phenoxide	-1.74[e]	0.46
MpNPPS					
PNPS	Pyridines w/ phenolates	-0.99[f]	Pyridines w/ phenolates	-1.24[f]	0.8
DEpNPP	Phenoxide	-0.51[e]	Phenoxide	-1.83[e]	0.28

a. From ref. S18.
b. From ref. S19.
c. From ref. S20.
d. From J. Zalatan and D. Herschlag, unpublished results.
e. From ref. S11.
f. From ref. S21.

Table S6. β_{lg}-Values in Solution for AP Substrates

Substrate	*Nucleophile*	β_{lg}	β_{lg} *in water*
PNPP	Water	-1.23[h]	-1.23
PNPPS	Water	-1.15[i]	-1.15
b(pNP)P	Hydroxide	-0.8[j]	-0.52[k]
MpNPP	Hydroxide	-0.8[j]	-0.52[k]
MpNPPS			
PNPS	Water	-1.23[l]	-1.23
DEpNPP	Phenoxide	-0.51[m]	0.00[n]

a. From ref. S18.
b. From ref. S20.
c. From J. Zalatan and D. Herschlag, unpublished results.
d. Obtained using p_{xy}(diester) = 0.016; $p_{xy} = \Delta\beta_{lg} / \Delta pK_{Nuc}$, from ref. S22 and S13.
e. From ref. S23.
f. From ref. S21.
g. Obtained using p_{xy}(triester) = 0.044; $p_{xy} = \Delta\beta_{lg} / \Delta pK_{Nuc}$, from ref. S24.

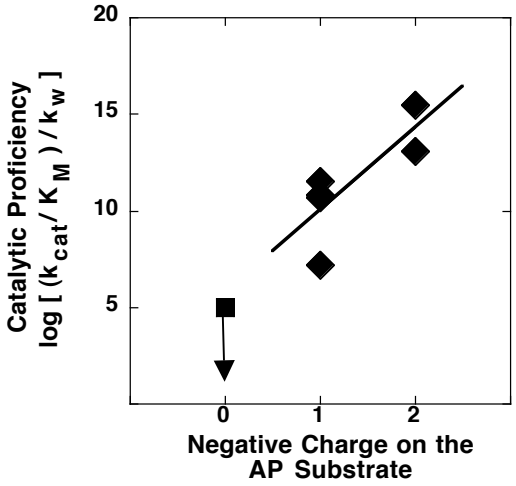

Figure S1. Correlation of the R166S AP catalytic proficiency with the total charge on the substrate. The solid line represents the best fit to the data with a slope of 5.5 kcal/ mol per unit charge and an $R^2 = 0.63$. The square symbol with the arrow denotes the upper limit for the R166S AP catalytic proficiency for dEpNPP, and was not included in the fit.

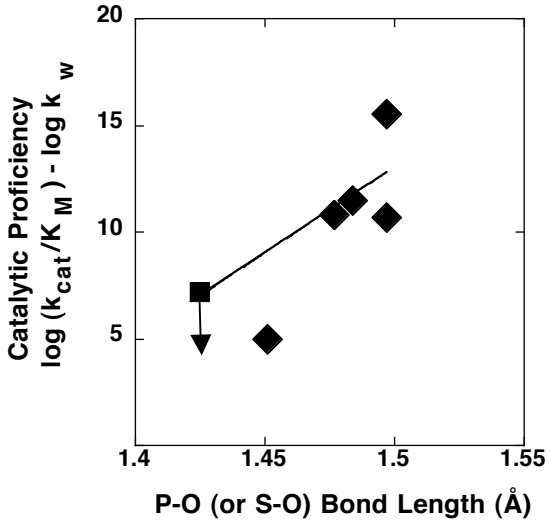

Figure S2. Correlation of the R166S AP catalytic proficiency with the P-O (S-O for pNPS) bond length for the non-bridging bond of the AP substrate. The solid line represents the best fit to the data with an $R^2 = 0.63$. The square symbol with the arrow denotes the upper limit for the R166S AP catalytic proficiency for dEpNPP, and was not included in the fit. Bond lengths are from reference S17.

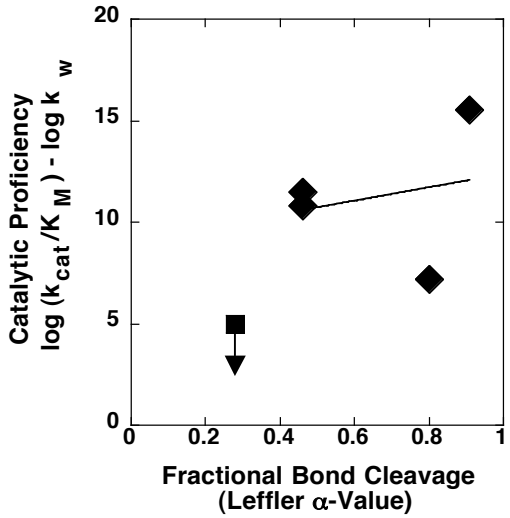

Figure S3. Correlation of the R166S AP catalytic proficiency with the solution fractional bond cleavage for each AP substrate. The solid line represents the best fit to the data R^2 = 0.05. The square symbol with the arrow denotes the upper limit for the R166S AP catalytic proficiency for dEpNPP, and was not included in the fit.

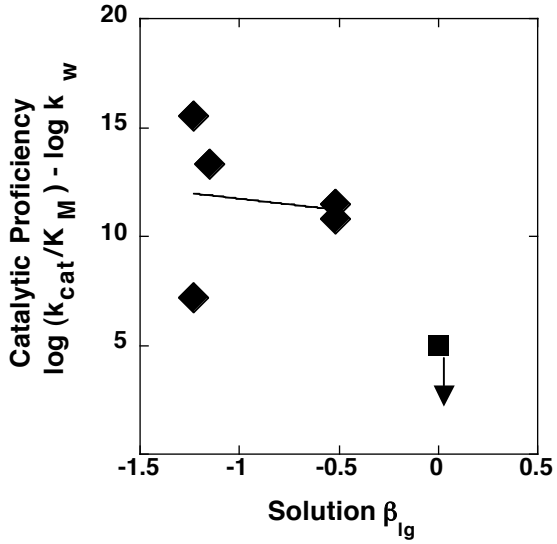

Figure S4. Correlation of the R166S AP catalytic proficiency with the nonenzymatic hydrolysis blg value for each AP substrate. The solid line represents the best fit to the data $R^2 = 0.05$. The square symbol with the arrow denotes the upper limit for the R166S AP catalytic proficiency for dEpNPP, and was not included in the fit.

Supporting References:

S1. Liang, C.; Allen, L. C. *J. Am. Chem. Soc.* **1987**, *109*, 6449.
S2. Frey, P. A.; Sammons, R. D. *Science*, **1985**, *228*, 541.
S3. (a) Cohn, M.; Hu, A. *J. Am. Chem. Soc.* **1980**, *102*, 913; (b) Jarvest, R. L; Lowe, G. *J. Chem. Soc. Chem. Commun.* **1979**, p. 364.
S4. Benkovic, S. J.; Benkovic, P. A. *J. Am. Chem. Soc.* **1966,** *88*, 5504
S5. O'Brien, P. J.; Herschlag, D. *J. Am. Chem. Soc.* **1999,** *121*, 11022
S6. See: http://www.neb.com.
S7. See: http://www.novagen.com.
S8. Cheng, H.; Nikolic-Hughes, I.; Wang, J.H.; Deng, H.; O'Brien, P.J.; Wu, L.; Zhang, Z.Y.; Herschlag, D.; Callender, R. *J. Am. Chem. Soc.* **2002**, *124*, 11295.
S9. O'Brien, P. J.; Herschlag, D. *J. Am. Chem. Soc.* **1998**, *120*, 12369.
S10. Catrina, I.E.; Hengge, A.C. *J. Am. Chem. Soc.* **1999**, *121*, 2156.
S11. Ba-Saif, S.A.; Davis, A.M.; Williams, A. *J. Org. Chem.* **1989**, *54*, 5483.
S12. Chin, J.; Banaszczyk, M.; Jubian, V.; Zou, X. *J. Am. Chem. Soc.* **1989**, *111*, 186.
S13. Kirby, A.; Younas, M. *J. Chem. Soc. B.* **1970**, p.1165.
S14. O'Brien, P.J; Herschlag, D. *Biochemistry* **2001**, *40*, 5691
S15. Herschlag, D,; Piccirilli, J.A.; Cech, T.R. *Biochemistry* **1991**, *30*, 4844.
S16. Hay, R.W.; Govan, N. *Polyhedron* **1996**, *15*, 2381.
S17. Cambridge Structural Database. See http://www.ccdc.cam.ac.uk.
S18. Kirby, A. J.; Varvoglis, A. G. *J. Am. Chem. Soc.* **1967**, *89*, 415.
S19. Bourne, N.; Williams, A. *J. Org. Chem.* **1984**, *49*, 1200.
S20. Hollfelder, F.; Herschlag, D. *Biochemistry* **1995**, *34*, 12255.
S21. Hopkins, A.; Day, R. A.; Williams, A. *J. Am. Chem. Soc.* **1983**, *105*, 6062.
S22. Herschlag, D.; Jencks, W. P. *J. Am. Chem. Soc.* **1989**, *111*, 7587.
S23. Nikolic-Hughes, I; Rees, D. C.; Herschlag, D. *J. Am. Chem. Soc.* **2004**, *126*, 11814.
S24. Kahn, S. A.; Kirby, A. J. *J. Chem. Soc. (B)* **1970**, p. 1172.